JOURNAL OF OPTOELECTRONICS AND ADVANCED MATERIALS Vol. 10, No. 7, July 2008, p. 1716 - 1721

Magnetic structure at zigzag edges of bilayer ribbons

EDUARDO V. CASTRO[a,*], N. M. R. PERES[b], J. M. B. LOPES DOS SANTOS[a]
[a]*CFP and Departamento de Física Faculdade Ciências, Universidade do Porto, P-4169-007 Porto, Portugal*
[b]*CFP and Departamento de Física Faculdade Ciências, Universidade do Minho, P-4710-057, Braga, Portugal*

We study the edge magnetization of bilayer graphene ribbons with zigzag edges. The presence of flat edge-state bands at the Fermi energy of undoped bilayer, which gives rise to a strong peak in the density of states, makes bilayer ribbons magnetic at the edges even for very small on-site electronic repulsion. Working with the Hubbard model in the Hartree Fock approximation we show that the magnetic structure in bilayer ribbons with zigzag edges is ferromagnetic along the edge, involving sites of the two layers, and antiferromagnetic between opposite edges. It is also shown that this magnetic structure is a consequence of the nature of the edge states present in bilayer ribbons with zigzag edges. Analogously to the monolayer case, edge site magnetization as large as m≈0.2 μ_B (per lattice site) even at small on-site Hubbard repulsion U≈0.3 eV is realized in nanometer wide ribbons.

(Received April 1, 2008; accepted June 30, 2008)

Keywords: Bilayer ribbon, magnetic structure, Graphene

1. Introduction

Graphene, the two dimensional allotrope of carbon, has recently been attracting a great deal of attention. Since its isolation three years ago [1] a plethora of unusual and interesting properties has been revealed [2,3].From the point of view of fundamental physics, low-energy quasi-particles in graphene behave like massless Dirac fermions propagating at an effective velocity of light $v \approx 10^6 ms^{-2}$. A rather unusual physics is then observed, where the half-integer quantum Hall effect is a paradigmatic example [4,5] Graphene is also regarded with great expectations from the point of view of technological applications. Stability and ballistic transport on the submicrometer scale, even at room-temperature, make graphene based electronics a promising possibility.

The possibility of creating stacks of graphene layers with the accuracy of a single atomic layer, providing an extra dimension to be explored, is another advantage of graphene for electronic applications. Of particular interest to us is the double layer of graphene – the *bilayer*. Bilayer graphene has shown to have unusual electronic properties, though unexpectedly dissimilar to those exhibited by its single layer parent. The new type of integer quantum Hall effect observed in bilayer grapheme [6,7] which is induced by chiral parabolic bands, is an example of its uniqueness. From the point of view of applications, bilayer graphene is even more promising for some electronic devices. It has recently been shown that the band structure of bilayer graphene can be controlled externally by an applied electric field so that an electronic gap between the valence and conduction bands can be tuned in a controllable way [8-10]. This makes the bilayer graphene the only known semiconductor with a tunable energy gap and may open the door for potential applications on atomic-scale electronic devices [11].

Among the uncommon features of monolayer graphene we find the rather different behavior of the two possible (perfect) terminations: *zigzag* and *armchair*. While zigzag edges support localized states, armchair edges do not [12-14]. These edge states occur at zero energy, the same as the Fermi level of undoped graphene, meaning that low energy properties may be substantially altered by their presence. The self-doping phenomenon [15], the edge magnetization with consequent gap opening in graphene nanoribbons [16], and half-metallicity [17] are examples of edge states driven effects.

The presence of zero energy edge states at zigzag edges of bilayer graphene has recently been confirmed assuming a first nearest-neighbor tight-binding model [18]. Two families of edge states has been found to coexist in the bilayer: monolayer edge states, with finite amplitude on a single plane; and bilayer edge states, with finite amplitude on both planes, and with an enhanced penetration into the bulk. As in single layer graphene, bilayer edge states show up in the electronic spectrum as flat bands at zero energy – the Fermi energy of undoped bilayer. These non-dispersive bands gives rise to a strong peak in the density of states right at the Fermi energy, which brings about the question of spontaneous magnetic ordering due to electron-electron interactions.

In the present paper we study the magnetic structure of zigzag bilayer graphene ribbons induced by electron-electron interactions, which are included through the Hubbard model. Working within the Hartree Fock approximation we show that due to the presence of edge states, which induce a strong peak in the density of states at the Fermi energy, zigzag bilayer ribbons show edge magnetization even for very small on-site electronic repulsion. Moreover, it is shown that the spin configuration is ferromagnetic along the edge, with parallel spins occurring on both layers, and

antiferromagnetic between opposite ribbon edges. Such a magnetic ordering can be interpreted as being a consequence of the edge state structure in bilayer graphene.

The paper is organized as follows: in Sec. we present the model and the mean field decoupling used here; for a better interpretation of our results we review briefly in Sec. the edge states for non-interacting zigzag bilayer ribbons; in Sec. we present and discuss the results of this work; we close with conclusions in Sec. .

2. Model and field treatment

The study of the magnetic structure in *AB*–stacked bilayer graphene given here is based on the ribbon geometry with zigzag edges shown in Fig. *0.1*. We use labels 1 and 2 for the top and the bottom layers, respectively, and labels *Ai* and *Bi* for each of the two sublattices in layer *i*. Each four-atom unit cell (parallelograms in Fig. *0.1*) has integer indices *m* (longitudinal) and *n* (transverse) such that $m\mathbf{a}_1+n\mathbf{a}_2$ is its position vector, where $\mathbf{a}_1=a(1,0)$ and $\mathbf{a}_2=a(1,-\sqrt{3})/2$ are the basis vectors and $a\approx 2.46$Å is the lattice constant. The simplest model one can write to describe non-interacting electrons in *AB*-stacked bilayer is the first nearest-neighbor tight-binding model given by,

$$H_{TB}=\sum_{i=1}^{2} H_{TB,i}+H_{\perp}, \tag{1}$$

with,

$$H_{TB,i}=-t\sum a^{t}_{i,\sigma}(m,n)[b_{i,\sigma}(m,n)+[b_{i,\sigma}(m-1,n)+$$

$$b_{i,\sigma}(m,n-1)]+h.c. \tag{2}$$

$$H_{\perp}=-t_1\sum a^{t}_{1,\sigma}(m,n)b_2(m.n)+h.c., \tag{3}$$

where $a_{i,\sigma}(m,n)$ [$b_{i,\sigma}(m,n)$] is the annihilation operator for the state in sublattice *Ai* (*Bi*), *i*=1,2, at position (*m*,*n*), and spin σ=↑,↓. The first term on the right hand side of Eq. (1) describes in-plane hopping, $t\approx 2.7eV$, while the second term parametrizes the inter-layer coupling, $t_{\wedge}/t\le 1$. In order to examine the magnetic polarization due to electron-electron interactions we add the Hubbard term to Eq.1. The total Hamiltonian describing the bilayer system reads,

$$H=H_{TB}+H_U, \tag{4}$$

where H_U represents the on-site Coulomb interaction,

$$H_U=U\sum_{i=1}^{2}\sum_{m,n}[a^{\dagger}_{i,-}(m,n)a_{i,-}(m,n)a^{\dagger}_{i,-}(m,n)a_{i,-}(m,n)$$
$$+b^{\dagger}_{i,-}(m,n)b_{i,-}(m,n)b^{\dagger}_{i,-}(m,n)b_{i,-}(m,n)] \tag{5}$$

The Hubbard model is a good starting point to study magnetism whenever the density of states at the Fermi energy is large enough to produce effective screening of the Coulomb interaction. This is true for the clean bilayer, where a finite density of states at the neutrality point produces some amount of screening in the system [19]. It is certainly the case in the presence of zigzag edges, where the density of states peak at the Fermi energy implies very effective screening.

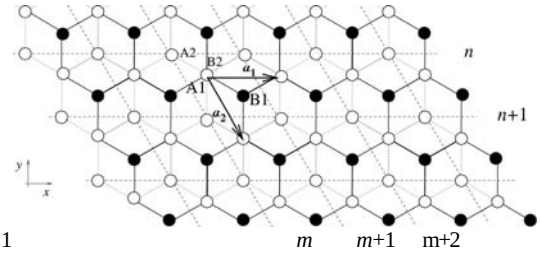

Fig. 0.1. Ribbon geometry with zigzag edges for bilayer graphene.

The system Hamiltonian in Eq. (4) is treated here within mean-field theory. In the Hartree Fock approximation the mean-field version of Eq. (4) reads,

$$H_{MF}=H_{TB}+H_U^{MF}, \tag{6}$$

with

$$H_U^{M*F}=U\sum_{i=1}^{2}\sum_{m,n,s}[\tilde{n}_{A*i,-s}(m,n)a^{\dagger}_{i,s}(m,n)a_{i,s}(m,n),$$
$$+\tilde{n}_{B*i,-s}(m,n)b^{\dagger}_{i,s}(m,n)b_{i,s}(m,n)] \tag{7}$$

where $\tilde{n}_{\Gamma i,\sigma}(m,n)$ is the electronic density for spin σ=↑,↓ at the site of sublattice Γ=*A*,*B* and layer *i*=1,2 of the cell (*m*,*n*). The electronic spin densities $\tilde{n}_{\Gamma i,\sigma}(m,n)$ have to be determined self-consistently through,

$$\tilde{n}_{A*i,s}(m,n)=\left\langle a^{\dagger}_{i\sigma}(m,n)a_{i,\sigma}(m,n)\right\rangle_{MF} \tag{8}$$

$$\tilde{n}_{B*i,s}(m,n)=\left\langle b^{\dagger}_{i\sigma}(m,n)b_{i,\sigma}(m,n)\right\rangle_{MF} \tag{9}$$

where the average $\langle\ \rangle_{MF}$ is done with the mean-field Hamiltonian in Eq. (6). Quantum fluctuations, which are ignored within mean-field theory, are expected to reduce the magnetic moments but not to change significantly the overall magnetic structure. As a further approximation we

assume that the self-consistent solution of Eqs. (8) and (9) is *m* independent, i.e.,

$$\tilde{n}_{A^*i,s}(m,n) \equiv \tilde{n}_{A^*i,s}(n) = \frac{1}{L}\sum_m \tilde{n}_{A^*i,s}(m,n) \quad (10)$$

$$\tilde{n}_{B^*i,s}(m,n) \equiv \tilde{n}_{B^*i,s}(n) = \frac{1}{L}\sum_m \tilde{n}_{B^*i,s}(m,n), \quad (11)$$

where L is the longitudinal ribbon length. We can justify this approximation here because we are mainly interested on the study of edge magnetization when edge states are present, and, as we will see in Sec. III, edge states are homogeneous along the edge. Note, however, that we keep the sublattice index in Eqs. (10) and (11), meaning that we can still have in-cell inhomogeneity.

Without loss of generality we assume that the ribbon in Fig. *0.1* has N unit cells in the transverse cross section (y direction) with $n \in \{0,\ldots,N-1\}$, and we use periodic boundary conditions along the longitudinal direction (x direction). Noting the translational invariance of the ribbon along the x direction, and having Eqs. (10) and (11) in mind, it is easy to diagonalize Hamiltonian (6) with respect to the m index just by Fourier transform along the longitudinal direction, $H = \sum_k H_k$, with H_k given by,

$$H_k = H_{TB,k} + H^{MF}_{U,k}, \quad (12)$$

where,

$$H_{TB,k} = -t\sum_{i=1}^{2}\sum_{n,\sigma} a_{i,\sigma}(k,n)\left[(1+e^{ik})b_{i,\sigma}(k,n) + b_{i,\sigma}(k,n-1)\right] - t_\perp \sum_{n,\sigma} a^\dagger_{1,\sigma}(k,n) b_{2,\sigma}(k,n) + h.c \quad (13)$$

and,

$$H^{M^*F}_{U,k} = U\sum_{i=1}^{2}\sum_{n,\sigma}\left[\tilde{n}_{A^*i,-\sigma}(n) a^\dagger_{i,\sigma}(k,n) a_{i,\sigma}(k,n) + \tilde{n}_{B^*i,-s}(n) b^\dagger_{i,s}(k,n) b_{i,s}(k,n)\right] \quad (14)$$

with self-consistent spin densities given by Eqs. (10) and (11), which can be rewritten as,

$$\tilde{n}_{A^*i,s}(n) = \left\langle a^\dagger_{i\sigma}(k,n) a_{i,\sigma}(k,n)\right\rangle_{MF} \quad (15)$$

$$\tilde{n}_{B^*i,s}(n) = \left\langle b^\dagger_{i\sigma}(k,n) b_{i,\sigma}(k,n)\right\rangle_{MF} \quad (16)$$

All conclusions presented in Sec. regarding the magnetic structure of zigzag bilayer ribbons are drawn by solving Eqs. (12-16).

3. Edge states in the non-interacting limit

It is shown in Sec IV. that the results for the edge magnetization of zigzag bilayer ribbons are a consequence of the edge state structure found in this system [18]. In this section we briefly review the main features of bilayer edge states for U=0 in Eq.(4), i.e., in the absence of interactions.

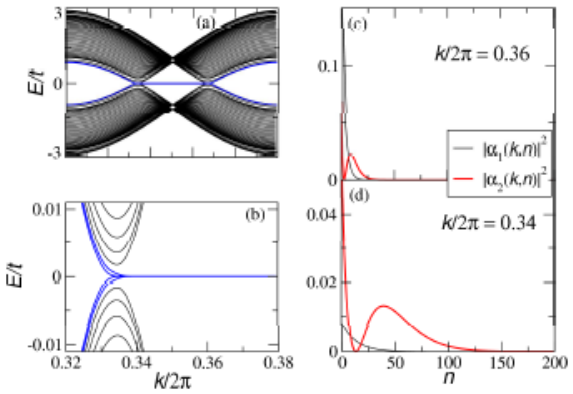

Fig. 0.2. (Color online) (a) - Energy spectrum for a graphene bilayer ribbon with zigzag edges for N=400. (b) - Zoom in of panel (a). (c) - Charge density of the edge states at $k/2\pi$=0.36. (d) - The same as in (c) at $k/2\pi$=0.364. The interlayer coupling was set to $t_\perp/t$=0.2 in all panels.

The band structure of a bilayer ribbon with zigzag edges is shown in Fig. *0.2* (a) for N=400, obtained by numerically solving Eq. (13). We can see the partly flat bands at E=0 for k in the range $2\pi/3 \le ka \le 4\pi/3$, corresponding to four edge states, two per edge. The zoom shown in Fig. *0.2* (b) for $ka \approx 2\pi/3$ clearly shows that there are four flat bands.

In order to understand the spatial structure of edge states in bilayer graphene we solve the Schrödinger equation, $H_{TB,k}|\mu,k\rangle = E_{\mu,k}|\mu,k\rangle$, for $E_{\mu,k}$=0, where μ labels the eigenstate index including spin. First we note that Hamiltonian $H_{TB,k}$ in Eq. (13) effectively defines a 1D problem in the transverse direction of the ribbon. It is then possible to write any eigenstate $|\mu,k\rangle$ as a linear combination of the site amplitudes along the cross section

$$|\mu,K\rangle = \sum_n \sum_{i=1}^{2}\left[\alpha_i(k,n)|a_i k,n,\sigma\rangle + \beta_i(k,n)|b_i,k,n,\sigma\rangle\right] \quad (17)$$

where the four terms per n refer to the four atoms per unit cell, to which we associate the one-particle states $|c_i,k,n,\sigma\rangle = c^\dagger_{i,\sigma}(k,n)|0\rangle$, with $c_{i,\sigma} = a_{i,\sigma}, b_{i,\sigma}$, spin σ=↑,↓, and i=1,2. To account for the finite width of the ribbon we require the following boundary conditions,

$$\alpha_1(k,N)=\alpha_2(k,N)=\beta_1(k,-1)=\beta_2(k,-1)=0. \quad (18)$$

After solving the Shrödinger equation for zero energy and the boundary conditions in Eq. (18) we find four possible eigenstates per k, where the only nonzero coefficients for each of them are given by [18]:

$$\begin{cases} \alpha_1(k,n)=0 \\ \alpha_2(k,n)=\alpha_2(k,0)D_k^n e^{-i\frac{ka}{2}n} \end{cases} \quad (19)$$

$$\begin{cases} \alpha_1(k,n)=\alpha_1(k,0)D_k^n e^{-i\frac{ka}{2}n} \\ \alpha_2(k,n)=-\alpha_1(k,0)D_k^{n-1}\frac{t_\perp}{t}e^{-i\frac{ka}{2}(n-1)}\left(n-\frac{D_k^2}{1-D_k^2}\right) \end{cases} \quad (20)$$

$$\begin{cases} \beta_1(k,n)=\beta_1(k,N-1)D_k^{n'}e^{i\frac{ka}{2}n'} \\ \beta_2(k,n)=0 \end{cases} \quad (21)$$

$$\begin{cases} \beta_1(k,n)=\beta_2(k,N-1)D_k^{n'-1}\frac{t_\perp}{t}e^{i\frac{ka}{2}(n'-1)}(n'-\frac{D_k^2}{1-D_k^2}) \\ \beta_2(k,n)=\beta_2(k,N-1)D_k^{n'}e^{i\frac{ka}{2}n'} \end{cases} \quad (22)$$

where $D_k=-2\cos(ka/2)$ and $n=N-n'-1$, with $n'\in\{0,\ldots,N-1\}$. As is easily seen, the coefficients in Eqs. (20-26) give convergent wave functions only if $2\pi/3<ka<4\pi/3$, in which case they represent zero energy states localized at the surface – edge states – and provide an explanation for the four flat zero energy bands in Fig. *0.2* (a) and (b). Note, however, that the solutions given by Eqs. (20-26) are exact eigenstates only for semi infinite systems, where the boundary conditions given in Eq. (18) are fully satisfied. In a finite ribbon overlapping of the four edge states leads to a slight dispersion and non-degeneracy. Nevertheless, as long as the ribbon width is sufficiently large, this effect is only important at $ka\approx 2\pi/3$ and $ka\approx 4\pi/3$ where the localization length is large enough for the overlapping to be appreciable [14]. For completeness we give the normalization constants appearing in Eqs. (20-26),

$$|\alpha_2(k,0)|^2=|\beta_1(k,N-1)|^2 = 1-D_k^2, \quad (23)$$

$$|\alpha_1(k,0)|^2=|\beta_2(k,N-1)|^2 = \frac{(1-D_k^2)^3}{(1-D_k^2)^2+t_\perp^2/t^2}. \quad (24)$$

An example of the charge density associated with Eq. (22) is shown in panels (c) and (d) of Fig. *0.2* for $t_\perp/t=0.2$, where the $|\alpha_1(k,n)|^2$ dependence can also be seen as the solution given by Eq. (20) for $|\alpha_2(k,n)|^2$, apart from a normalization factor. Of particular interest to understand the magnetic structure due to interaction effects is the fact that edge states in zigzag bilayer graphene are such that at one edge they live only on sublattice A whereas at the opposite edge they live on sublattice B.

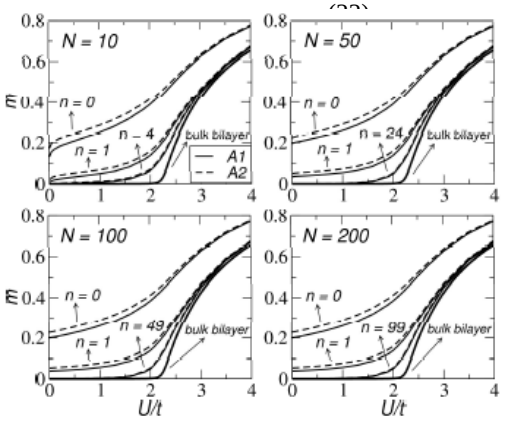

Fig. 3. Dependence of the magnetization $m=\tilde{n}_{Ai,\uparrow}-\tilde{n}_{Ai,\downarrow}$, with $i=1,2$, on the interaction parameter U for different ribbon widths N. The shown magnetizations were computed at sites $n=0$, $n=1$, and at the middle of the ribbon. Solid lines are for the upper layer ($i=1$) and dashed lines for the bottom layer ($i=2$). The result for graphite double sheet (bulk bilayer) is also shown.

4. Results and discussion

In Fig. *3* the results for the local magnetization $m=\tilde{n}_{Ai,\uparrow}-\tilde{n}_{Ai,\downarrow}$, for $i=1,2$, are shown as a function of the Hubbard parameter U for different ribbon widths N. For each ribbon width we have computed the local magnetization at sites of the A sublattice belonging to cells $n=0$, $n=1$, and right at the middle of the ribbon (see Fig. *0.1*). The first conclusion we can draw is that sites near the edge get polarized even for very small U, while sites in the middle of the ribbon behave like bulk bilayer [20]. Another interesting feature shown in Fig. *3* is that at the considered edge the magnetization of $A2$ sites is larger than that of $A1$ sites, an asymmetry that vanishes away from the edge. We will come back to this below. As regards the B sublattice its magnetization (not shown in Fig. *3*) is always similar to the bulk result even right at the edge ($n=0$). However, when we move to the opposite edge, the A and B sublattices change roles: B sites at the opposite edge get polarized for very small U while A sites show the bulk result. The conclusion then is that edge magnetization involving different sublattices at opposite edges is

showing up in zigzag bilayer ribbons, even for very small U. In particular we get $m \approx 0.2\mu_B$ right at the edge for $U=0.1t \approx 0.3eV$, similar to what is found in graphene [12].

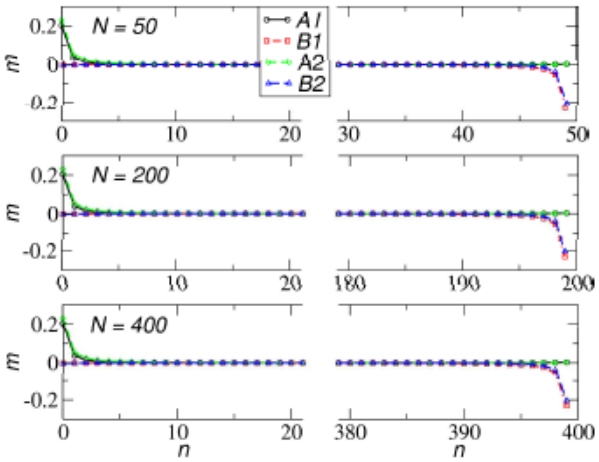

Fig. 0.4. (Color online) Magnetization $m=\tilde{n}_{\Gamma i,\uparrow}-\tilde{n}_{\Gamma i,\downarrow}$ *along the ribbon cross section for the* $\Gamma i=A1,A2,B1,B2$. *Three different ribbon widths were considered: N = 50, 200, 400 from top to bottom. The interaction parameter was set to U=0.1t.*

A better understanding of the edge magnetization is achieved by fixing U and plotting the local magnetization $m=\tilde{n}_{\Gamma i,\uparrow}-\tilde{n}_{\Gamma i,\downarrow}$ across the ribbon section for $\Gamma i=A1,A2,B1,B2$. This is done in Fig. *0.4* for different ribbon widths and for a fixed interaction parameter $U=0.1t$. As is clearly seen, for such a small interaction only the edges are polarized. Moreover, the edge magnetization is opposite on opposite edges – *antiferromagnetic arrangement across the ribbon*. Also, we can see that at the edge starting with cell $n=0$ only sublattice A has a finite magnetization, whereas at the opposite edge only sublattice B has non-vanishing magnetization. Finally, it is also apparent that at each edge the non-zero sublattice magnetization has same sign in both layers – *ferromagnetic arrangement along the edge*. These observations are consistent with first-principles density-functional calculations of the magnetic structure of graphitic fragments (infinite number of layers) [21].

We have seen in Sec.III that bilayer edge states have the following property: at the edge starting with $n=0$ they live only on sublattice A, while at the opposite edge they live only on sublattice B, as given by Eqs. (20-26). The above results for the edge magnetization may therefore be attributed to the polarization of edge states in order to reduce on-site Coulomb energy. This interpretation also provides an explanation for the layer difference in local magnetization. As mentioned before, it can be seen in Fig. *3* that the magnetization at $A2$ sites is higher than at $A1$ sites for the edge starting with $n=0$. If we recall Eqs. (20) and (22) for the wave function amplitudes at the considered edge we immediately see that while the two edge state families contribute to $A2$ only one has finite amplitude at $A1$ sites. The same is true for $B1$ and $B2$ sites, in agreement with Eqs. (24) and (26). As regards the antiferromagnetic polarization between edge states living in opposite edges, it guarantees a ground state with zero total magnetization, as it is known to be the case for the half-filled Hubbard model.

Finally we note that edge magnetization gives rise to a finite gap at the Fermi level, in complete analogy to monolayer graphene [16]. Half-metallicity has been predicted for zigzag single layer ribbons due to the edge magnetization and the presence of a finite gap [17]. We expect that bilayer ribbons also become half-metallic, with an extra switching capability owing to the effect of a perpendicular electric field [9,10].

5. Conclusions

We have studied the edge magnetization in bilayer graphene ribbons with zigzag edges. The presence of flat edge-state bands at the Fermi energy of undoped bilayer, which gives rise to a strong peak in the density of states, makes bilayer ribbons magnetic at the edges even for very small on-site electronic repulsion. Using the Hubbard model in the Hartree Fock approximation we have shown that the magnetic structure in bilayer ribbons with zigzag edges is ferromagnetic along the edge, involving sites of the two layers but belonging to the same sublattice, and antiferromagnetic between opposite edges and involving sites of different sublattices. This magnetic structure is a consequence of the nature of the edge states present in bilayer ribbons with zigzag edges.

Acknowledgments

E.V.C. acknowledges the financial support of Fundação para a Ciência e a Tecnologia through Grant No. SFRH/BD/13182/2003. E.V.C., N.M.R.P., and J.M.B.L.S. acknowledge financial support from POCI 2010 via project PTDC/FIS/64404/2006.

References

[1] K. Novoselov, A. Geim, S. Morozov, D. Jiang, Y. Zhang, S. Dubonos, I. Grigorieva, A. Firsov, Science **306,** 666 (2004).
[2] A.K.Geim, K. Novoselov, Nature Materials **6**, 183 (2007).
[3] M. I. Katsnelson, Materials Today **10**, 20 (2007).
[4] K. Novoselov, A. Geim, S. Morozov, D. Jiang, M. Katsnelson, I. Grigorieva, S. Dubonos, A. Firsov, Nature **438,** 197 (2005).
[5] Y. Zhang, Y.-W. Tan, H. L. Stormer, P. Kim, Nature **438,** 201 (2005).
[6] E. McCann, V. I. Fal'ko, Phys. Rev. Lett. **96**, 086805 (2006).

[7] K. S. Novoselov, E. McCann, S. V. Morozov, V. I. Falko, M. I. Katsnelson, U. Zeitler, D. Jiang, F. Schedin, A. K. Geim, Nature Physics **2**, 177 (2006).
[8] T. Ohta, A. Bostwick, T. Seyller, K. Horn, and E. Rotenberg, Science **313,** 951 (2006).
[9] E. V. Castro, K. S. Novoselov, S. V. Morozov, N. M. R. Peres, J. M. B. Lopes dos Santos, J. Nilsson, F. Guinea, A. K. Geim, A. H. Castro Neto, cond-mat/0611342.
[10] J. B. Oostinga, H. B. Heersche, X. Liu, A. F Morpurgo, L. M. K. Vandersypen, arXiv:0707.2487vl [cond-mat.mes-hall].
[11] J. Nilsson, A. H. C. Neto, F. Guinea, N. M. R. Peres, cond-mat/0607343.
[12] M. Fujita, K. Wakabayashi, K. Nakada, K. Kusakabe, J. Phys. Soc. Jpn. **65**, 1920 (1996).
[13] K. Nakada, M. Fujita, G. Dresselhaus, M. S. Dresselhaus, Phys. Rev. B **54**, 17954 (1996).
[14] K. Wakabayashi, M. Fujita, H. Ajiki, M. Sigrist, Phys. Rev. B **59**, 8271 (1999).
[15] N. M. R. Peres, F. Guinea, A. H. Castro Neto, Phys. Rev. B **73**, 125411 (2006).
[16] Y.-W. Son, M. L. Cohen, S. G. Louie, Phys. Rev. Lett. **97**, 216803 (2006).
[17] Y.-W. Son, M. L. Cohen, S. G. Louie, Nature **444,** 347 (2006).
[18] E. V. Castro, N. M. R. Peres, J. M. B. Lopes dos Santos, A. H. Castro Neto, F. Guinea, arXiv:0707.3819vl [cond-mat.mes-hall].
[19] X.-F. Wang and T. Chakraborty, cond-mat/0611635.
[20] The Hartree Fock result *m vs. U* for infinite bilayer graphene is very close to that for graphene single layer, where a finite critical interaction parameter $U_c \sim 2.2$Hs needed to have a broken symmetry ground state. Despite biayer's finite density of states, which implies a mean field $U_c = 0$, the fact that $t\pm$ <C *t* originates a monolayer like *m vs. U*, except for the discontinuity in the first derivative at $U_c \sim 2.2t$ which is removed. Indeed, the critical U_c was shown to be essentially the same for graphene and graphite within RPA [22].
[21] H. Lee, Y.-W. Son, N. Park, S. Han, and J. Yu, Phys. Rev. B **72**, 174431 (2005).
[22] N. M. R. Peres, M. A. N. Araujo, and D. Bozi, Phys. Rev. B **70**, 195122(2004).

*Corresponding author: evcastro@fc.up.pt